Theoretical characterization of 5-oxo, 7-oxo and 5-oxo-7-amino[1,2,4]triazolo[1,5-*a*]pyrimidines †

Jose A. Dobado,* Sonja Grigoleit and José Molina Molina ‡

Grupo de Modelización y Diseño Molecular, Instituto de Biotecnología, Campus Fuentenueva, Universidad de Granada, 18071-Granada, Spain. Fax: +34-958-243186; E-mail: dobado@ugr.es

Received (in Cambridge, UK) 30th March 2000, Accepted 2nd June 2000
Published on the Web 17th July 2000

Accurate *ab initio* calculations at the B3LYP/6-311+G** level have been performed on anionic and neutral structures of 4,5-dihydro-5-oxo[1,2,4]triazolo[1,5-*a*]pyrimidine, 4,7-dihydro-7-oxo[1,2,4]triazolo[1,5-*a*]pyrimidine, and 4,5-dihydro-7-amino-5-oxo[1,2,4]triazolo[1,5-*a*]pyrimidine compounds. The quality of the theoretical results has been tested against the experimental X-ray structures for the three most stable neutral forms, yielding very good agreement. The electronic properties of the anionic forms have been evaluated by means of the atoms in molecules theory (AIM) and electrostatic potential analyses, allowing the rationalization of the coordination mode preferences observed experimentally for the anions. Moreover, a theoretical study of the tautomerism for the neutral forms has also been made, by energetic, geometrical and NMR chemical shift (GIAO method) calculations. The results gave the protonated forms at the N^4 atom as the most stable ones, corroborated by the experimental geometries and the NMR data. In addition, the preferred coordination mode at the N^3 atom, against N^1 or the carbonyl oxygen, is also discussed.

I. Introduction

Triazolopyrimidine derivatives show a large variety of interactions with metal ions, as has been very recently reviewed.[1] The bonding with transition metal ions seems to be responsible for the use of 5-methyl-7-hydroxy[1,2,4]triazolo[1,5-*a*]pyrimidine as a photographic stabilizer by interaction between a silver cation and the unprotonated nitrogen of the ligand.[2,3] For these heterocyclic ligands, tautomerism plays a determinant role in its reactivity and coordination modes. In this context, theoretical studies on the 5-methyl-7-oxo[1,2,4]triazolo[1,5-*a*]-pyrimidine tautomers identified a keto form as the most stable one.[4]

Studies focusing on the possible M···M interactions[5–7] and M–L bonding characteristics,[8] including the structures and theoretical analyses of several triazolopyrimidine ligands,[8,9,10] have been performed by our group. In this context, transition metal complexes of 5-oxo, 7-oxo, and 5-oxo-7-amino derivatives of 1,2,4-triazolo[1,5-*a*]pyrimidine are suitable structures with possible biological activity against Gram(+) and Gram(−) bacteria.[11] The goal of the present work is to perform a detailed theoretical characterization, including an atoms in molecules (AIM)[12,13] topological analysis of the bonding properties of the ligands; in order to rationalize the reactivity and coordination modes of their complexes with the transition metal complexes.

Although the MO theory, by wavefunction analysis, is able to give a qualitative picture of the bonding nature in many cases, a topological analysis of the observable electron density, $\rho(r)$, is used in this paper to produce a quantitative description of the bonding properties of the aforementioned ligands. Moreover, several topological analyses of the electron density have been recently performed by our group.[14–16] Calculations for the anionic and neutral triazolopyrimidine derivatives, depicted in Scheme 1, have been made in the present work.

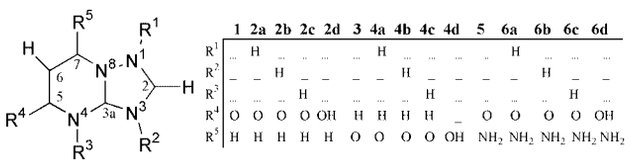

	1	2a	2b	2c	2d	3	4a	4b	4c	4d	5	6a	6b	6c	6d
R^1	...	H	...	...	...	...	H	...	...	...	...	H	...	...	...
R^2	_	_	H	_	_	_	_	H	_	_	_	_	H	_	_
R^3	...	...	...	H	...	...	...	...	H	...	...	...	...	H	...
R^4	O	O	O	O	OH	H	H	H	H	_	O	O	O	O	OH
R^5	H	H	H	H	H	O	O	O	O	OH	NH_2	NH_2	NH_2	NH_2	NH_2

Scheme 1 Compounds studied with the atom numbering.

II. Methods

A. General methods

All calculations have been carried out using the GAUSSIAN98 package[17] of programs. All the geometries have been fully optimized and all the stationary points on the hypersurface have been characterized by harmonic frequency analysis. Structures **1**, **2b–d**, **3** and **4a–d** were restricted to C_s symmetry. The B3LYP/6-311+G** theoretical level was used to study all the compounds (**1**–**6**). The NMR chemical shifts were calculated with the Gauge independent atomic orbitals (GIAO) method[18] within the GAUSSIAN98 program,[17] using the tetramethylsilane (TMS) signal as a reference for the ^{1}H and ^{13}C chemical shifts and the dimethylformamide (DMF) signal for the ^{15}N shifts.

Atoms in molecules theory (AIM) analyses have been performed with the AIMPAC series of programs,[19] using the B3LYP/6-311+G** density as input as was described in the AIM theory.[12,13] The $\nabla^2\rho(r)$ contour-map representations have been produced using the MORPHY98 program.[20] The atomic charges have been calculated with the AIMPAC series of programs,[19] by integration over the basin of every atom in the Bader framework.

B. Overview of the $\rho(r)$ topology

The topology of the electronic charge density, $\rho(r)$, as described by Bader,[13] is an accurate mapping of the chemical concepts of atom, bond, and structure. The principal topological properties are summarized in terms of their critical points (CP).[12,13] The

† Tables S1 and S2, and Figs. S1–S3 are available as electronic supplementary information. For direct electronic access see http://www.rsc.org/suppdata/p2/b0/b002527p/

‡ Professor José Molina Molina passed away on the 13th June 2000.

Table 1 Total and relative energies for all the structures at the B3LYP/6-311+G** theoretical level

	E_{tot}/hartree	ΔE_r[a]/kcal mol^{-1}		E_{tot}/hartree	ΔE_r[a]/kcal mol^{-1}		E_{tot}/hartree	ΔE_r[a]/kcal mol^{-1}
1	−486.755 317 3		**3**	−486.768 467 8		**5**	−542.135 703 8	
2a	−487.248 016 7	31.6	**4a**	−487.277 846 8	9.5	**6a**	−542.629 606 7	35.8
2b	−487.277 798 3	12.9	**4b**	−487.287 571 1	3.4	**6b**	−542.660 518 9	16.4
2c	−487.298 306 2	0.0	**4c**	−487.292 979 6	0.0	**6c**	−542.686 677 3	0.0
2d	−487.291 089 1	4.5	**4d**	−487.283 604 8	5.9	**6d**	−542.680 986 7	3.6

[a] Relative energy with respect to the most stable **c** tautomers.

nuclear positions behave topologically as local maxima in $\rho(r)$. A bond critical point (BCP) is found between each pair of nuclei, which are considered to be linked by a chemical bond, with two negative curvatures, λ_1 and λ_2, and one positive, λ_3, denoted as (3,−1) CP. The ellipticity, ε, of a bond is defined by means of the two negative curvatures in a BCP, in eqn. (1).

$$\varepsilon = (\lambda_1/\lambda_2) - 1, \text{ where } |\lambda_2| < |\lambda_1| \quad (1)$$

The ring CPs are characterized by a single negative curvature. Each (3,−1) CP generates a pair of gradient paths[12] which originate at a CP and terminate at neighbouring attractors. This gradient path defines a line through the charge distribution linking the neighbouring nuclei. Along this line, $\rho(r)$ is a maximum with respect to any neighbouring line. Such a line is referred to as an atomic interaction line.[12,13] The presence of an atomic interaction line in such equilibrium geometry satisfies both the necessary and sufficient conditions that the atoms be bonded together. The Laplacian of the electronic charge density, $\nabla^2\rho(r)$, describes two extreme situations. In the first, $\rho(r)$ is locally concentrated ($\nabla^2\rho(r) < 0$) and in the second it is locally depleted ($\nabla^2\rho(r) > 0$). Thus, a value of $\nabla^2\rho(r) < 0$ at a BCP is unambiguously related to a covalent bond, showing that a sharing of charge has taken place. While in a closed-shell interaction, a value of $\nabla^2\rho(r) > 0$ is expected, as found in noble gas repulsive states, ionic bonds, hydrogen bonds, and van der Waals molecules. Bader has also defined a local electronic energy density, $E_d(r)$, as a functional of the first order density matrix (eqn. (2)),

$$E_d(r) = G(r) + V(r) \quad (2)$$

where the $G(r)$ and $V(r)$ terms correspond to a local kinetic and potential energy density, respectively.[12] The sign of the $E_d(r)$ determines whether accumulation of charge at a given point r is stabilizing ($E_d(r) < 0$) or destabilizing ($E_d(r) > 0$). Thus, a value of $E_d(r) < 0$ at a BCP presents a significant covalent contribution and, therefore, a lowering of the potential energy associated with the concentration of charge between the nuclei.

III. Results and discussion

Accurate theoretical calculations have been performed for the different tautomers of three triazolopyrimidine skeletons, in the anionic and neutral forms: 5-oxo[1,2,4]triazolo[1,5-*a*]-pyrimidine derivatives (**1** and **2a**–**d**), 7-oxo[1,2,4]triazolo[1,5-*a*]-pyrimidine derivatives (**3** and **4a**–**d**) and 5-oxo-7-amino-[1,2,4]triazolo[1,5-*a*]pyrimidine derivatives (**5** and **6a**–**d**), see Scheme 1. The numerical results are illustrated in Tables 1–3, and Figs. 1 and 2, and supplementary Figs. S1 to S3. Figs. 1 and 2 and S1 show the different structures studied (**1**–**6**), including the geometrical parameters and electrostatic potential values. For the different neutral tautomers, the most stable ones correspond to **2c**, **4c**, and **6c**; where the hydrogen is bonded to N^4 (see Table 1).

For the 5-oxo derivatives the tautomers with the hydrogen at N^1 (**2a** and **6a**) are extremely unstable with relative energies (compared to **2c** and **6c**, respectively) larger than 30 kcal mol^{-1}. Moreover, the N^3 tautomers are also unfavourable structures with relative energies of around 15 kcal mol^{-1}. However, the

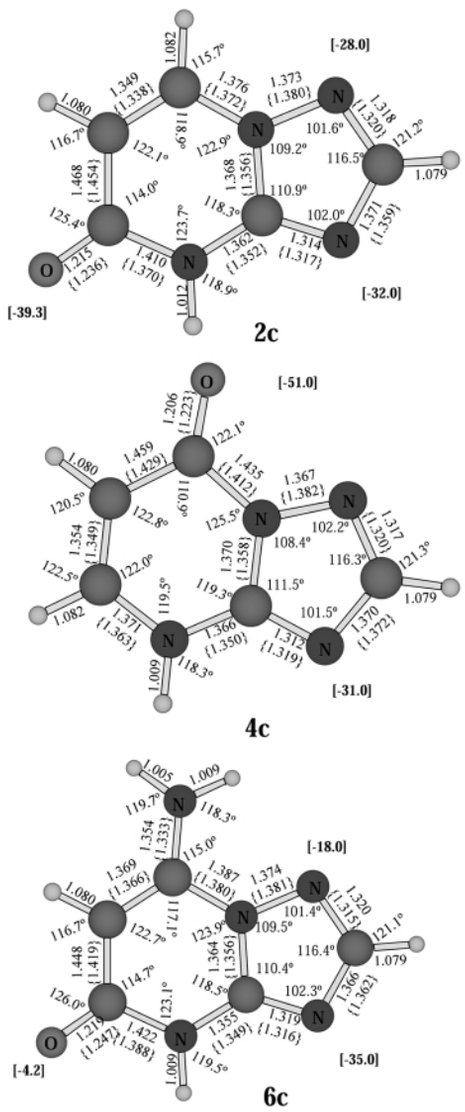

Fig. 1 Theoretical structures **2c**, **4c** and **6c**, including geometries {X-ray data in braces}[21] and symmetry, together with the minimum values of the electrostatic potentials [in brackets] calculated at the B3LYP/6-311+G** level.

hydroxylated tautomers (**2d** and **6d**) are the following in stability after the N^4 tautomers, with relative energies of around 5 kcal mol^{-1}. A change in the stability order was observed for the 7-oxo derivatives, the energy differences being smaller than the corresponding 5-oxo ones ($N^4 < N^3 < OH < N^1$, with a relative energy value of 9.5 kcal mol^{-1} for the N^1).

The most stable tautomer for the **2**, **4** and **6** series corresponded to the N^4 one (**2c**, **4c** and **6c**), in agreement with those determined from X-ray data.[11,22] Figs. 1, 2 and S1 show the geometrical data of the structures studied, and for **2c**, **4c** and **6c** the X-ray data are also included for comparison. The theoretical data are in good agreement with the experimental data. The main differences appeared in the carbonyl group description, yielding shorter C=O and longer C–N and C–C bonds

Table 2 AIM charges and the NMR chemical shifts,[a] at the B3LYP/6-311+G** level

	Charge	δ(ppm)	Charge	δ(ppm)	Charge	δ(ppm)	Charge	δ(ppm)	Charge	δ(ppm)
	1		**2a**		**2b**		**2c**		**2d**	
N^1	−0.74	161.4	−0.71	44.0	−0.66	176.1	−0.67	182.7	−0.66	180.3
C^2	0.94	159.6	1.02	158.1	1.01	140.2	0.95	160.5(152.6)	0.96	164.1
N^3	−1.08	120.8	−1.02	167.7	−1.14	22.1	−1.04	121.0	−1.04	136.9
C^{3a}	1.29	167.1	1.36	164.1	1.41	153.5	1.39	156.8(150.0)	1.33	161.4
N^4	−1.11	128.6	−1.07	155.5	−1.08	118.0	−1.13	35.0	−1.13	127.6
C^5	1.31	175.9	1.34	170.9	1.33	170.2	1.34	162.6(161.0)	1.13	169.5
C^6	−0.03	114.8	0.01	119.6	0.01	120.6	0.01	114.0(108.0)	0.02	102.4
C^7	0.38	134.5	0.35	133.9	0.36	136.9	0.40	142.4(136.9)	0.45	143.6
N^8	−0.84	101.8	−0.82	59.1	−0.83	88.3	−0.84	104.8	−0.82	124.4
O^5	−1.20		−1.12		−1.13		−1.13		−1.09	
H(@N,@O)[b]			0.42	7.2	0.45	7.0	0.44	7.8(13.3)	0.59	5.7
H^2	0.02	7.4	0.10	7.9	0.11	7.4	0.09	7.9(8.11)	0.08	8.3
H^6	0.02	5.6	0.07	6.1	0.07	6.2	0.08	6.1(6.16)	0.08	6.5
H^7	0.04	7.6	0.07	7.4	0.09	7.7	0.11	8.1(8.62)	0.12	8.6
	3		**4a**		**4b**		**4c**		**4d**	
N^1	−0.69	172.0	−0.77	45.8	−0.63	183.6	−0.63	188.6	−0.69	150.7
C^2	0.94	156.6	1.02	145.9	1.01	139.4	0.96	157.8(151.8)	0.96	162.7
N^3	−1.10	127.8	−1.01	149.1	−1.15	28.0	−1.06	124.0	−1.03	142.8
C^{3a}	1.28	168.5	1.35	161.5	1.40	155.5	1.37	156.1(151.0)	1.31	163.5
N^4	−1.13	113.4	−1.08	125.8	−1.11	88.6	−1.17	3.2	−1.08	168.8
C^5	0.49	156.2	0.48	162.9	0.45	158.9	0.41	138.6(141.0)	0.57	160.4
C^6	−0.10	100.5	−0.04	109.1	−0.05	112.5	−0.01	108.4(99.1)	0.02	95.8
C^7	1.26	164.9	1.26	158.3	1.29	158.4	1.34	158.9(156.6)	1.03	160.5
N^8	−0.77	139.0	−0.77	105.5	−0.76	127.6	−0.76	135.8	−0.84	116.7
O^7	−1.18		−1.15		−1.12		−1.10		−1.10	
H(@N,@O)[b]			0.48	10.1	0.45	7.6	0.44	7.3	0.61	7.2
H^2	0.01	7.6	0.11	8.0	0.11	7.6	0.08	8.0(8.25)	0.08	8.5
H^5	−0.02	7.8	0.05	8.5	0.05	8.0	0.07	7.2(8.02)	0.06	8.8
H^6	−0.00	5.3	0.06	6.2	0.06	6.2	0.07	5.9(5.96)	0.07	6.5
	5		**6a**		**6b**		**6c**		**6d**	
N^1	−0.75	142.4	−0.71	36.2	−0.69	159.8	−0.69	163.1	−0.69	158.5
C^2	0.95	158.7	1.01	159.3	1.01	139.6	0.96	159.1(152.0)	0.96	162.4
N^3	−1.08	118.6	−1.02	171.2	−1.14	21.1	−1.04	118.8	−1.04	133.8
C^{3a}	1.31	166.1	1.36	163.1	1.42	151.6	1.40	156.1(150.2)	1.35	161.4
N^4	−1.11	120.2	−1.07	153.8	−1.08	112.9	−1.13	28.7	−1.13	104.9
C^5	1.29	176.7	1.32	172.3	1.31	170.6	1.31	162.4(162.1)	1.10	171.1
C^6	−0.04	90.2	0.00	96.6	−0.01	91.6	−0.01	84.6(77.6)	0.01	78.2
C^7	0.76	149.8	0.75	151.5	0.80	150.1	0.85	152.6(149.0)	0.92	153.7
N^8	−0.85	92.7	−0.81	55.3	−0.83	79.1	−0.85	92.6	−0.83	105.3
O^5	−1.24		−1.13		−1.14		−1.14		−1.10	
N^7	−1.06	67.0	−1.04	63.9	−1.08	63.6	−1.11	54.6	−1.12	−50.4
H(@N,@O)[b]			0.41	7.0	0.45	6.9	0.44	7.4(12.04)	0.59	5.4
H^2	0.02	7.4	0.10	8.0	0.11	7.4	0.08	7.8(8.08)	0.07	8.2
H^6	0.00	4.9	0.05	5.4	0.05	5.3	0.06	5.1(4.96)	0.06	5.6
H^{7a}	0.35	2.5	0.39	3.2	0.40	3.4	0.41	4.0(7.47)	0.41	4.3
H^{7b}	0.39	4.3	0.38	2.8	0.41	4.3	0.44	5.3(7.47)	0.44	5.7

[a] Experimental ^{13}C shifts in parentheses obtained from ref. 10 for **2c** and **4c** and ref. 24 for **6c**; the ^1H and ^{13}C signals of TMS, and the ^{15}N signal of DMF were used for reference. [b] Hydrogen bonded to the N^1, N^3, N^4 and O atoms for the **a**, **b**, **c** and **d** tautomers, respectively.

than the corresponding theoretical values (*i.e.* 1.215 *vs.* 1.236 Å for C=O, 1.468 *vs.* 1.454 Å for C–C and 1.410 *vs.* 1.370 Å for C–N bonds in compound **2c**).

The geometrical features gave overall planar structures except for the N^1 tautomers (**2a** and **6a**). Structures **1**, **2b–d**, **3** and **4a–d** have C_s symmetry, while **5** and **6b–d** displayed planar ring geometries without symmetry (C_1), due to the NH_2 group at C^7. The pronounced instability of the N^1 tautomers in the 5-oxo compound (**2a** and **6a**) is explained by a ring deformation due to the pyramidalization of the N^1 atom, yielding N^1–C^2 and N^1–N^8 distances larger than in their corresponding anions, the N^3 and N^4 tautomers (see Figs. 1, 2 and S1).

For the 7-oxo tautomer **4a**, the N^1 atom became planar and the overall structure of the molecule remained C_s, by the adjacent carbonyl group effect, yielding also shorter N^1–C^2 and N^1–C^8 bonds. An overall comparison of the theoretical geometries of the different tautomers **2a–d**, **4a–d** and **6a–d** with the experimental data concluded that the N^4 tautomer was the one detected by X-ray (*i.e.* the N^3–C^2 single bond distance is *ca.* 1.37 Å and the N^3=C^{3a} double bond distance is *ca.* 1.31 Å).

The good agreement of the theoretical with the experimental geometries displays the quality of the B3LYP/6-311+G** level for the description of these systems, including the anions **1**, **3** and **5**, where no experimental data were available. To test the theoretical electronic properties, calculations of the NMR chemical shifts were carried out for all the structures, including ^1H, ^{13}C and ^{15}N shifts. The data are shown in Table 2.

A comparison of the experimental data for **2**, **4** and **6** with the theoretical values of the different tautomers gives **2c**, **4c** and **6c** as the experimentally observed tautomers, also in solution. Both ^1H and ^{13}C theoretical shifts matched the experimental

Table 3 The electron charge density, $\rho(r)$, its $\nabla^2\rho(r)$, ellipticity, ε, of structures **1**, **2c**,**d**, **3**, **4c**,**d**, **5** and **6c**,**d** for the different BCPs at the B3LYP/6-311+G** level

	$\rho(r)$/e a_o^{-3}	$\nabla^2\rho(r)$/e a_o^{-5})	ε	$\rho(r)$/e a_o^{-3}	$\nabla^2\rho(r)$/e a_o^{-5}	ε	$\rho(r)$/e a_o^{-3}	$\nabla^2\rho(r)$/e a_o^{-5}	ε
	1			**2c**			**2d**		
N^1–C^2	0.349	−0.960	0.234	0.357	−0.927	0.250	0.350	−0.946	0.219
C^2–N^3	0.340	−1.026	0.161	0.322	−0.947	0.129	0.334	−1.002	0.137
N^3–C^{3a}	0.339	−1.034	0.180	0.369	−1.154	0.230	0.361	−1.133	0.220
C^{3a}–N^4	0.355	−1.111	0.172	0.320	−0.949	0.190	0.338	−1.045	0.153
N^4–C^5	0.317	−0.946	0.104	0.285	−0.767	0.088	0.364	−1.098	0.190
C^5–C^6	0.267	−0.657	0.138	0.275	−0.707	0.142	0.294	−0.797	0.190
C^6–C^7	0.330	−0.959	0.324	0.333	−0.969	0.332	0.326	−0.938	0.304
C^7–N^8	0.308	−0.723	0.090	0.301	−0.710	0.037	0.313	−0.707	0.066
N^8–N^1	0.342	−0.575	0.109	0.345	−0.586	0.100	0.354	−0.623	0.104
C^{3a}–N^8	0.297	−0.768	0.146	0.320	−0.877	0.210	0.298	−0.779	0.166
C^5–O^5	0.386	−0.419	0.077	0.412	−0.299	0.096	0.303	−0.461	0.030
	3			**4c**			**4d**		
N^1–C^2	0.354	−0.975	0.241	0.359	−0.946	0.252	0.342	−0.919	0.204
C^2–N^3	0.336	−1.009	0.159	0.321	−0.940	0.131	0.340	−1.027	0.149
N^3–C^{3a}	0.346	−1.069	0.199	0.371	−1.160	0.237	0.355	−1.108	0.205
C^{3a}–N^4	0.345	−1.083	0.162	0.316	−0.917	0.194	0.348	−1.100	0.156
N^4–C^5	0.339	−0.998	0.117	0.303	−0.727	0.072	0.347	−0.963	0.119
C^5–C^6	0.311	−0.855	0.268	0.329	−0.947	0.330	0.298	−0.800	0.202
C^6–C^7	0.291	−0.774	0.225	0.279	−0.721	0.161	0.318	−0.913	0.300
C^7–N^8	0.276	−0.726	0.078	0.271	−0.710	0.061	0.322	−0.868	0.181
N^8–N^1	0.350	−0.607	0.102	0.350	−0.607	0.093	0.357	−0.632	0.108
C^{3a}–N^8	0.299	−0.789	0.174	0.319	−0.894	0.224	0.293	−0.714	0.148
C^7–O^7	0.397	−0.381	0.082	0.419	−0.216	0.102	0.315	−0.474	0.074
	5			**6c**			**6d**		
N^1–C^2	0.347	−0.946	0.229	0.354	−0.908	0.244	0.348	−0.926	0.218
C^2–N^3	0.342	−1.037	0.166	0.326	−0.965	0.135	0.336	−1.013	0.143
N^3–C^{3a}	0.336	−1.018	0.174	0.366	−1.142	0.219	0.358	−1.120	0.210
C^{3a}–N^4	0.360	−1.131	0.183	0.326	−0.983	0.197	0.342	−1.070	0.158
N^4–C^5	0.313	−0.926	0.096	0.278	−0.738	0.079	0.359	−1.112	0.178
C^5–C^6	0.269	−0.660	0.166	0.282	−0.729	0.203	0.300	−0.813	0.252
C^6–C^7	0.323	−0.916	0.368	0.319	−0.892	0.362	0.312	−0.870	0.318
C^7–N^8	0.313	−0.847	0.148	0.301	−0.836	0.097	0.316	−0.876	0.123
N^8–N^1	0.339	−0.558	0.108	0.343	−0.577	0.103	0.350	−0.602	0.104
C^{3a}–N^8	0.295	−0.746	0.137	0.319	−0.847	0.202	0.298	−0.750	0.158
C^5–O^5	0.386	−0.427	0.076	0.409	−0.341	0.095	0.301	−0.469	0.024
C^7–N^7	0.303	−0.910	0.125	0.326	−0.996	0.168	0.328	−0.993	0.160

data for **2d**, **4d** and **6d**. Moreover, the carbonyl ^{13}C shift was characteristic of an amide arrangement.

Although the theoretical ^1H and ^{13}C shift values give support to N^4 being the favoured tautomers, the shifts for the other tautomers are in the same range. This is not the case for the ^{15}N shifts, which gave four different sets of values, allowing the preferred tautomer to be unambiguously assigned.

All the above considerations indicate the N^4 tautomers to be the most stable in the gas-phase, solid state and solution. However, the N^3 tautomer for compound **4** is of similar stability (3.4 kcal mol^{-1}), compatible with the related 5-methyl derivatives.[4] Moreover, the energy difference of the enol tautomers is small (<6 kcal mol^{-1}) for **2**, **4** and **6**. In an effort to gain information on the coordination properties of these ligands and the different anions, a detailed investigation of the electronic properties was made with AIM and the electrostatic potential analyses.

The complexity of this coordination analysis required the use of different electronic parameters, one of the most widely used being atomic charges. However, additional approaches such as the molecular orbitals (shape and symmetry) or the electrostatic potentials were also followed.[10,23]

In the present study, a topological analysis of different electronic parameters was performed, including the electron density and the electrostatic potentials. The AIM charges, listed in Table 2, indicate a net electron accumulation on the different heteroatoms, for compounds **1**–**6**, yielding a high charge accumulation (with similar values) for the N^3, N^4 and O atoms. Additionally, the net charge on the NH_2 nitrogen for **5** and **6** is in the same range (*ca.* −1.1 electrons). The coordination at the protonated heteroatoms was rejected, and therefore the remaining analysis was performed on the unprotonated ones. In further studies, analysis of the closed-shell d^{10} type transition metal complexes of these ligands will be carried out, where the coordination mode is mainly a sigma type.

The AIM data are summarized in Table 3 and Figs. S2 and S3, for compounds **1**, **3**, **5**, **2c**, **4c** and **6c**. The data for all the structures are available as Supplementary Material.† Figs. S2 and S3 show a network of electronic charge concentration around the heterocyclic skeleton. Moreover, the nature of the different bonds is characteristic of a strong covalent bond with different multiple bonding degrees. The $\rho(r)$ values at the BCPs are higher than 0.3 e a_o^{-3} with high and negative $\nabla^2\rho(r)$ values, together with negative electronic density values $E_d(r)$, indicating a typical covalent bond. In addition, the ellipticity, ε, values are in the range *ca.* 0.1–0.4, compatible with different bonding multiplicity and some degree of electronic delocalization. Figs. S2 and S3 clearly show the different $\nabla^2\rho(r)$ maxima around the heteroatoms. Furthermore, the unprotonated nitrogens displayed one non-bonded maximum in the molecular plane compatible with the σ-coordination mode observed for the transition metal complexes for these kinds of ligands.[1] The carbonyl oxygen showed two non-bonded maxima on

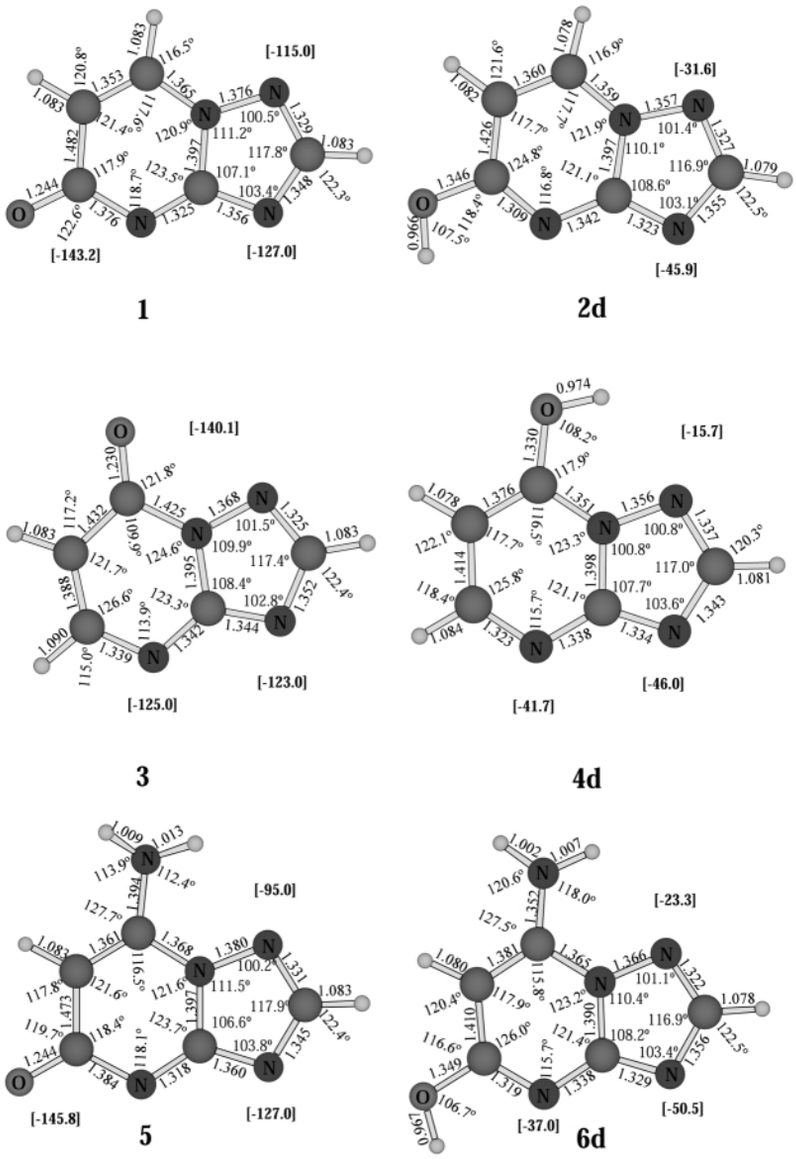

Fig. 2 Theoretical structures **1**, **3**, **5**, **2d**, **4d** and **6d**, including geometries and symmetry, together with the minimum values of the electrostatic potentials [in brackets] calculated at the B3LYP/6-311+G** level.

the molecular plane, compatible with a bent coordination with a metal–oxygen–carbon angle of *ca.* 116°, which is rarely observed.[8]

The numerical values of the $\nabla^2\rho(r)$ maxima are summarized in Table S2 for the different heteroatoms, of the anionic structures **1**, **3** and **5**, and the neutral ones **2c**,**d**, **4b**–**d** and **6c**,**d**. The maxima on N^1, N^3 and N^4 have similar characteristics, with $\rho(r)$ values of *ca.* 0.56 e a_o^{-3} and $\nabla^2\rho(r)$ of *ca.* −2.5 e a_o^{-5} and located at *ca.* 0.4 Å from the nucleus.

For **1**, **3** and **5** the minimum values of the electrostatic potentials at the different positions are indicated in Figs. 1, 2 and S1, yielding larger values at N^3 and N^4 than at N^1. These values, together with the atomic charges, explain the preferred coordination mode of N^3 *vs.* N^1 positions.

Alternative coordination at N^1 and O^7 was also found experimentally for **3**, compatible with the higher electron localization at the $\nabla^2\rho(r)$ maxima. The maximum values of the charge concentration and the electrostatic potentials are observed for the two maxima at the carbonyl oxygen. However, O-coordination is rarely observed, which is in agreement with its bent disposition and higher $\nabla^2\rho(r)$ values (the maxima on O are *ca.* 0.34 Å and the $\nabla^2\rho(r)$ values *ca.* 4.8 e a_o^{-5} *vs.* 0.4 Å and −2.5 e a_o^{-5} on N). For **1**, **3** and **5** coordination at N^4 is also possible according to the theoretical results, compatible with the N^3 and N^4 coordination displayed in bidentate ligands.[1]

The N^4 tautomer is the most stable among the compounds **2**, **4** and **6**. The characteristics of the neutral compounds remained almost unchanged. There is a different kind of normal covalent bond character, clearly evident from Figs. S2 and S3 and Table 3.

For the N^4 tautomers, there is also a non-bonded maximum at the N^1 and N^3 atoms, together with the two maxima at oxygen, all in the molecular plane.

The numerical values for these maxima showed a large electron charge concentration, *ca.* 0.4 Å, from N^1 and N^3. However, the maximum at N^1 is slightly closer to the nucleus than in N^3 (0.388 *vs.* 0.392 Å for **2c**). Moreover, for these compounds, the atomic charge and the electrostatic potentials are larger in N^3 than in N^1, compatible with the preferred N^3 coordination observed experimentally.

IV. Conclusions

Accurate theoretical calculations for several triazolopyrimidine derivatives which can be used as synthesis ligands in transition metal complexes, have been performed, including a characterization of the most stable tautomers. The B3LYP/6-311+G**

level of theory reproduced in good agreement the experimental X-ray geometries. In the gas-phase the N^4 tautomer is the preferred one. Theoretical NMR chemical shifts have been calculated and a comparison with the experimental shifts also yielded the N^4 tautomer as the most stable one in solution for the compounds **2**, **4** and **6**. Moreover, the theoretical ^{15}N shifts allow unambiguous assignment of the preferred tautomer in solution.

The coordination analysis of the anionic species **1**, **3** and **5** and the neutral compounds **2**, **4** and **6** have been analysed by means of the topological properties of $\rho(r)$, $\nabla^2\rho(r)$, electrostatic potentials and AIM charges, concluding that the N^3 and N^4 are the preferred coordination centres for the anions. Moreover, for the neutral molecules, a similar analysis yielded the N^3 site as the preferred coordination mode.

Acknowledgements

This work was supported by the DGES project no. PB-97-0786-CO3-O2. S. G. acknowledges the Deutsche Forschungsgemeinschaft. Computing time has been provided by the University of Granada (Spain). We are grateful to Professor R. F. W. Bader for a copy of the AIMPAC package of programs. We thank David Nesbitt for reviewing the language of the English manuscript.

References

1 J. M. Salas, M. A. Romero, M. P. Sánchez and M. Quirós, *Coord. Chem. Rev.*, 1999, **193**–**195**, 1119.
2 E. J. Birr and Z. Wiss, *Photography*, 1952, **47**, 2.
3 E. J. Birr, *Chimica*, 1970, **24**, 125.
4 A. Koch, S. Thomas and E. Kleinpeter, *THEOCHEM*, 1997, **401**, 1.
5 J. El-Bahraoui, J. A. Dobado and J. Molina, *THEOCHEM*, 1999, **493**, 249.
6 J. El-Bahraoui, J. Molina and D. Portal, *J. Phys. Chem. A*, 1998, **102**, 2443.
7 J. A. R. Navarro, M. A. Romero, J. M. Salas, M. Quirós, J. El-Bahraoui and J. Molina, *Inorg. Chem.*, 1996, **35**, 7829.
8 J. A. R. Navarro, M. A. Romero, J. M. Salas, J. Molina and E. R. T. Tiekink, *Inorg. Chim. Acta*, 1998, **274**, 53.
9 S. Orihuela, M. P. Sánchez, M. Quirós, J. Molina and R. Faure, *J. Mol. Struct.*, 1997, **415**, 285.
10 M. Abul-Haj, J. M. Salas, M. Quirós, J. Molina and R. Faure, *J. Mol. Struct.*, 2000, **519**, 165.
11 J. A. R. Navarro, J. M. Salas, M. A. Romero, R. Vilaplana, F. Gonzalez-Vilchez and R. Faure, *J. Med. Chem.*, 1998, **41**, 332.
12 R. F. W. Bader, *Atoms in Molecules: a quantum theory*, Clarendon Press, Oxford, 1990.
13 R. F. W. Bader, *Chem. Rev.*, 1991, **91**, 893.
14 J. A. Dobado, H. Martínez-García, J. Molina and M. R. Sundberg, *J. Am. Chem. Soc.*, 2000, **122**, 1144.
15 J. A. Dobado, H. Martínez-García and J. Molina, *Inorg. Chem.*, 1999, **38**, 6257.
16 J. A. Dobado and J. Molina, *J. Phys. Chem. A*, 1999, **103**, 4755.
17 GAUSSIAN98, Revision A.6, M. J. Frisch, G. W. Trucks, H. B. Schlegel, G. E. Scuseria, M. A. Robb, J. R. Cheeseman, V. G. Zakrzewski, J. A. Montgomery, Jr., R. E. Stratmann, J. C. Burant, S. Dapprich, J. M. Millam, A. D. Daniels, K. N. Kudin, M. C. Strain, O. Farkas, J. Tomasi, V. Barone, M. Cossi, R. Cammi, B. Mennucci, C. Pomelli, C. Adamo, S. Clifford, J. Ochterski, G. A. Petersson, P. Y. Ayala, Q. Cui, K. Morokuma, D. K. Malick, A. D. Rabuck, K. Raghavachari, J. B. Foresman, J. Cioslowski, J. V. Ortiz, B. B. Stefanov, G. Liu, A. Liashenko, P. Piskorz, I. Komaromi, R. Gomperts, R. L. Martin, D. J. Fox, T. Keith, M. A. Al-Laham, C. Y. Peng, A. Nanayakkara, C. Gonzalez, M. Challacombe, P. M. W. Gill, B. Johnson, W. Chen, M. W. Wong, J. L. Andres, C. Gonzalez, M. Head-Gordon, E. S. Replogle and J. A. Pople, Gaussian, Inc., Pittsburgh, PA, 1998.
18 K. Wolinski, J. F. Hilton and P. Pulay, *J. Am. Chem. Soc.*, 1990, **112**, 8251.
19 F. W. Biegler-König, R. F. W. Bader and T.-H. Tang, *J. Comput. Chem.*, 1982, **3**, 317.
20 MORPHY98 a program written by P. L. A. Popelier with a contribution from R. G. A. Bone, UMIST, Manchester, UK, 1998.
21 X-Ray data of compound **6c** from ref. 21, and for **2c** and **4c** from ref. 11.
22 H. Orgueira, M. A. Haj, J. M. Salas, W. P. Jensen and E. R. T. Tiekink, *Z. Kristallogr. NCS*, 1999, **214**, 517.
23 J. M. Salas, M. A. Romero, M. P. Sánchez, M. Moreno, M. Quirós, J. Molina and R. Faure, *Polyhedron*, 1992, **11**, 2217.
24 H. Orgueira, M. A. Haj and J. M. Salas, unpublished results.